

Exploiting Capillary Sorbent Films for Air Revitalization aboard Spacecraft: Analysis of a Semi-Passive CO₂ Scrubber

Mark M. Weislogel,¹ Logan J. Torres,² Ryan M. Jenson,³
IRPI LLC, Portland, OR, 97201

John C. Graf⁴
NASA Johnson Space Center, Houston, TX, 77058

and

Lawrence A. Hand,⁵ Grace A. Belancik,⁶ Darrell L. Jan,⁷ and Julie A. Levri⁸
NASA Ames Research Center, Moffett Field, CA 94035

Liquid sorbents have provided a primary means for robust carbon dioxide (CO₂) control aboard submarines for decades. Unfortunately, such systems have not been adopted for use aboard spacecraft due to the fact that fine droplet sprays, thin falling films, and buoyancy-driven bubbly flows are not easily managed in the essentially gravity-free environments of orbiting spacecraft. Such applied engineering challenges have remained outstanding for the microgravity fluid physics community. As a work-around, in this research, a stable, silent capillary-driven ‘thin film’ is produced over a massively parallel network of open channels for both CO₂ uptake and degas functions in a microgravity environment. Following several quantified assumptions, simple analytical models of species, heat, mass, and momentum transport are invoked providing clear design guides for a future engineering demonstration of the approach aboard the International Space Station. For critical sorbent properties such as CO₂ capacity, effective diffusion rate, and concentration- and temperature-dependent viscosity, we provide the essential requirements of flow rate, size, shape, stability, power draw, and other aspects of the system. The results imply that a considerable reduction in system mass and volume is possible for the liquid sorbent approach for CO₂ scrubbing when compared to the current state of the art.

Nomenclature

α	= wedge channel half-angle	δ	= liquid sorbent diffusion layer thickness
α_t	= thermal diffusivity, $k/\rho c_p$	δ_{am}	= air mom. boundary layer thickness
a	= acceleration	δ_{at}	= air thermal boundary layer thickness
A	= cross flow area	δ_{ac}	= air CO ₂ boundary layer thickness
c_p	= specific heat	ϕ	= interface curvature angle, $\pi/2 - \alpha - \theta$
C	= concentration of CO ₂	f	= curvature function, $\sin \alpha / (\cos \theta - \sin \alpha)$
D	= liquid sorbent CO ₂ diffusion coefficient	F_A	= area function, $f^2 (\cos \theta \sin \phi / \sin \alpha - \phi)$
DEA	= Diethanolamine	h	= meniscus center line height
DGA	= Diglycolamine	h_{fg}	= latent heat of vaporization

¹ Principle Investigator, 2828 SW Corbett Ave., Suite 143.

² Engineer, 2828 SW Corbett Ave., Suite 143.

³ Lead Engineer, 2828 SW Corbett Ave., Suite 143.

⁴ Principle Investigator, Life Support Systems Branch, MC EC3.

⁵ Research Scientist, Experimental Aero-Physics Branch, MS 260-1.

⁶ Principle Investigator, Bioengineering Branch, MS 239-15.

⁷ Principle Investigator, Bioengineering Branch, MS 239-15.

⁸ CapiSorb PMSE, Flight Implementation Branch, MS 240A-3.

H	= meniscus height at entrance/exit	R	= wedge channel half-width
k	= thermal conductivity	S	= sorbent volumetric source/sink
L	= channel length	t	= time
μ	= dynamic viscosity	σ	= surface tension
\dot{m}	= mass flow rate of CO ₂	T	= temperature
MEA	= Monoethanolamine	U	= mean air flow velocity
ν	= frequency	V	= volume
P	= pressure	w	= z -component of velocity
θ	= liquid contact angle	W	= z -component average velocity
q	= heat	x	= wedge channel depth coordinate
Q	= liquid sorbent flow rate	y	= wedge channel lateral coordinate
ρ	= density	z	= wedge channel axial coordinate

I. Introduction

Controlled removal of carbon dioxide from the spacecraft crew habitat atmosphere is critical for crew health for all NASA missions. The International Space Station (ISS) currently uses the Carbon Dioxide Removal Assembly (CDRA), which relies on a packed bed of molecular sieve solid sorbent. CDRA has experienced many years of successful operation, despite certain performance issues.^{1,2} Various alternatives, as well as a next generation version of CDRA, are in development.³

One alternative is to employ liquid sorbent systems, as used on many submarines. The microgravity space environment, unlike submarines, requires special handling to control liquids. Various approaches to liquid control in microgravity include powered centrifuge,⁴ hollow fiber membranes,⁵ and use of capillary forces to hold the liquid in place.^{6,7} The ability to control liquids in microgravity applications is pivotal in leveraging high-capacity liquid sorbents that have proven to be essential to terrestrial industrial CO₂ removal applications. Additionally, liquid sorbent systems can be used in a continuous flow mode between CO₂ uptake and degassing components. This is a key advantage over current solid bed-based systems, due to the ability to provide relatively low but positively pressured product gas to downstream processors in a continuous mode.

In a safety-conservative environment such as the ISS, high-capacity CO₂ liquid sorbents such as monoethanolamine (MEA) and diglycolamine (DGA) require additional hazard controls beyond those employed in submarine and petroleum industry environments. On the ISS, the failure tolerant approach to prevent release of hazardous materials has traditionally been through the implementation of ‘levels of containment,’ based on the severity of the hazard. The levels of containment approach require concentric, independent, physical barriers in the design, where each barrier is able to contain the material through all worst-case environments. However, recent progress in demonstration of liquid control using surface tension and capillary action on ISS⁸⁻¹⁰ has resulted in allowance of alternatives to physical barriers during on-orbit operations (i.e., experiment setup, data collection, and tear-down) for liquids rated as ‘toxicity hazard level 1.’¹¹ Such migration toward acceptance of non-physical barriers for liquid control is exemplary of the forward-thinking that enables substantial advancements in technology efficiency and/or size reduction.

In this paper we briefly introduce the Liquid Amine Carbon-dioxide Removal (LACR) approach to CO₂ scrubbing aboard spacecraft, where the primary design challenge over similar terrestrial systems is one of addressing the unique challenges of microgravity fluid mechanics. We begin with a description of the elements of the design with the intent of replacing the passive role of gravity with that of surface tension. We then provide the dimensional limitations of such systems for stable operation aboard spacecraft. The analysis that follows considers the various time scales of most aspects of the species, momentum, and heat transport, and offers area, volume, and power expectations for the LACR approach for a candidate working sorbent. The work is summarized by a recipe for the analysis which may be further pursued for component- and system-level design, testing, performance analysis, and trade studies.

II. The LACR Approach

The LACR approach seeks to exploit capillary forces to establish stable thin film flows through which to efficiently absorb and desorb CO₂ through a largely silent passive process in a microgravity environment. A simplified representative cycle is shown in Fig. 1, where CO₂ absorber (Contactor) and desorber (Degasser) are pictured in simple serial operation. In this example, the Contactor functions at cabin pressure. A reversible pump and system control valve allow for slightly positive or negative gauge pressure operation in the Degasser. Though numerous stably contained capillary flows might be adopted,¹²⁻¹⁴ we exploit an interior corner flow approach of which a large literature

exists with key demonstrations performed aboard the ISS.^{9,14,15} The unit cell function of the interior corner (wedge) inherent in both Contactor and Degasser is identified and annotated in Fig. 2.

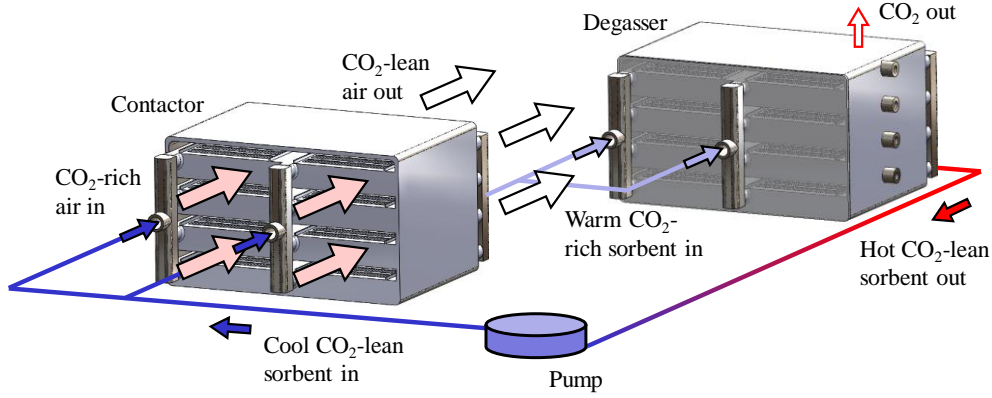


Figure 1. Simplified LACR System: fan-driven air through Contactor and heater-driven release of CO₂ in Degasser.

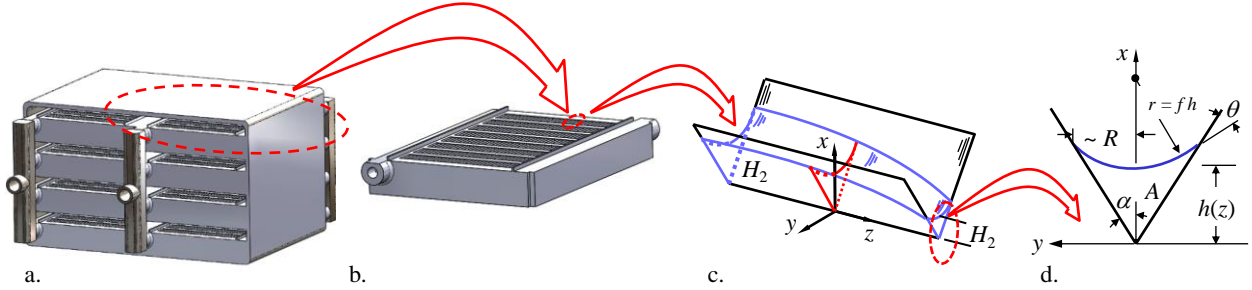


Figure 2. a. LACR Contactor or Degasser device from Fig. 1 with b. sub-deck, c. single open capillary wedge channel, and d. single channel cross section with relevant notation.

Both Contactor and Degasser possess massively parallel, open, capillary channels to form essentially thin flowing films. The films extract CO₂ from CO₂-rich cabin air into the CO₂-lean liquid sorbent in the Contactor and exhaust CO₂ from the CO₂-rich liquid sorbent to the headspace in the Degasser. It is the number of channels, their dimension, and performance that determines the performance envelope of the LACR system. Figure 2 illustrates that, using this approach, a single open wedge channel can mimic the role of gravity by combining the effects of surface tension, wetting, and channel geometry; as liquid is withdrawn from the wedge, a capillary under-pressure is created in the liquid, drawing the fluid from the entrance to the exit. In this way, such flows can occur essentially passively in the reduced acceleration environments aboard spacecraft. Because they can accommodate both microgravity and gravity conditions, such systems are ‘omni-gravitational’ and thus ground testable. The stability of capillary surfaces to background acceleration fields is long-established for simple geometries.^{17,18} For the wedge geometry of Fig. 2c, provided the Bond number criteria $Bo \equiv \rho a R L / \sigma \lesssim 1$ is satisfied, the flow across the channel will be fairly insensitive to background g -levels on the same order as on Earth, where $a = g_o = 9.8 \text{ m/s}^2$, as well as spacecraft flight perturbations or accelerations such as crew kickloads²⁴ ($a \leq 0.2g_o$ at modest frequencies $\nu > 1 \text{ Hz}$), docking²⁵ ($a < 10^{-2}g_o$), and thruster firings²⁶ ($a < 10^{-2}g_o$)—all of which are considered significantly less than g_o . Typical spacecraft orbit or coast acceleration levels are routinely $a \ll 10^{-4}g_o$, where LACR capillary channel flows are designed to be completely insensitive.

The thermophysical properties of the working fluids are critical to all aspects of the momentum, species, and heat transport. It can be shown for the purposes of assessing LACR system performance relevant to other methods of spacecraft CO₂ scrubbing that at least two figures of merit arise for the working fluid;

$$V_{liq} \approx \frac{\dot{m} \delta^2}{\rho_{liq} D \Delta C} \quad \text{and} \quad q \approx \frac{\dot{m} c_p \Delta T}{\Delta C}, \quad (1)$$

the former which provides a characteristic measure of the active liquid volume V_{liq} in circulation and the latter a measure of the power q required. For the above two metrics, the effective liquid film thickness, δ , is the only fluid system design parameter present. The working fluid properties dominate the performance primarily through the CO₂

uptake capacity ΔC and effective diffusion coefficient D . A competitive design will minimize both expressions in Eq. (1), while addressing the ever-present concerns of safety, reliability, compatibility, human factors, maintenance, mass, volume, cost, crew time etc.

III. LACR Analysis

The steady flow along a single open capillary wedge channel is represented schematically in Fig. 3. The notation for the transport analysis to follow is adopted in reference to Fig. 2c-d. As sketched in Fig. 3, CO₂-rich air at known temperature, pressure, relative humidity, and CO₂ concentration C_a is forced over the liquid free surface at a specified rate Q_a leading to known air momentum δ_{am} , concentration δ_{ac} , and thermal δ_{at} boundary layers. The maximum or characteristic CO₂ penetration depth in the liquid is δ . The instantaneous local CO₂ concentration in the liquid at the free surface, C_0 , depends the CO₂ concentration in the air that is in direct contact with it, C_{a0} , via an experimentally determined temperature-dependent solubility function. For physical and weakly reactive aqueous sorbents (including pure water), the dependence is nearly linear (Henry's law¹⁹) and $C_0 \approx C_{a0}$. In contrast, highly reactive sorbents (e.g. DGA) exhibit effective solubilities that are nonlinear and several orders of magnitude higher (e.g. $C_0 = 10^4 C_{a0}$ for a particular value of C_{a0}).^{20,28}

The CO₂-lean liquid sorbent of diffusion coefficient D absorbs CO₂ as the liquid is wicked along the channel driven by a negative capillary pressure gradient created by differing meniscus elevations H_1 and H_2 corresponding to the pressure difference of the liquid inlet and outlet, respectively. Note that the liquid is delivered to and removed from the wedge channel by a pump, but the flow across the channel is driven passively by capillary forces in an analogous manner to when significant gravity is present. For optimal performance, the channel dimensions must be chosen to maximize stability to physical perturbations, CO₂ uptake rate, and desired degree of CO₂ saturation, while minimizing liquid volume, flow rate, and system envelope. We repeat that maximizing CO₂ saturation minimizes the liquid volume through the contactor which in turn minimizes the power required to eventually degas the liquid, ref. Eq. (1). The concentration of CO₂ in the sorbent is $C = C(x,y,z)$. The liquid properties that most govern sorbent performance include surface tension σ , density ρ , dynamic viscosity μ , contact angle θ , CO₂ diffusion coefficient D , CO₂ saturation level at the inlet $C_{liq,i}$, and desired CO₂ saturation level at the outlet $C_{liq,o}$, where $\Delta C \equiv C_{liq,o} - C_{liq,i} \equiv C_o - C_i$. Such properties are functions of CO₂ saturation level, temperature, relative humidity, and relative concentration ratio if the sorbent is an aqueous mixture (i.e., DGA-water). Critical channel dimensions include channel height H , length L , and interior corner half-angle α , where channel half-width is $R \approx \delta \tan \alpha$. The steady axial meniscus centerline profile is given by $h(z)$.

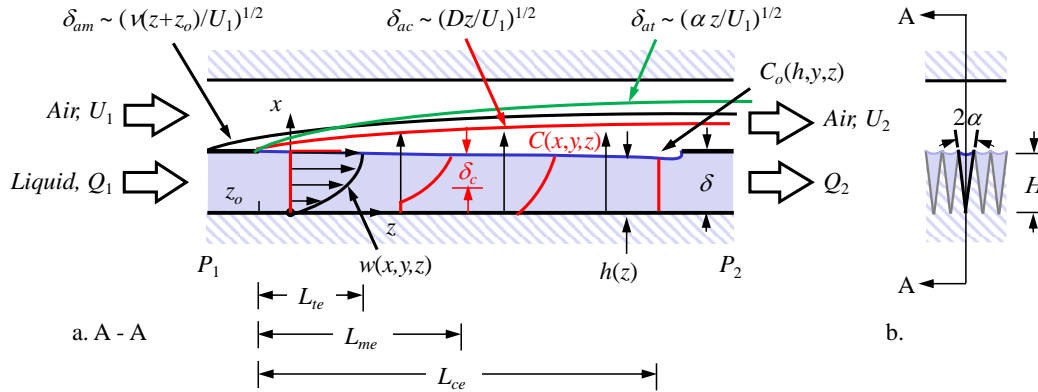


Figure 3. a. Schematic of transport in LACR Contactor with co-flow air and liquid sorbent left to right with b. cross-section view. Representative air boundary layers and liquid entrance lengths are identified along with the nearly flat liquid interface profile $h(z)$. Degasser transport may be addressed in a similar manner.

A. Assumptions

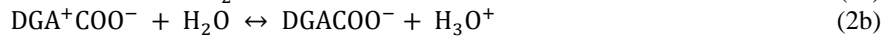
Practical fabrication and operation considerations drive the design. For example, excessively small flow passageways may improve performance via thinner films with higher transport rates, but such passageways are difficult to machine en masse and may lead to premature clogging in practice. We expect that our devices will be 3D-printed. With this method in mind, assuming a $\delta_c = 1$ mm thick CO₂ active liquid amine film (i.e., DGA) at $T = 20$ C

($\mu/\rho \sim 2 \cdot 10^{-7} \text{ m}^2/\text{s}$, $\alpha \sim 10^{-7} \text{ m}^2/\text{s}$, $D \sim 10^{-9} \text{ m}^2/\text{s}$) the characteristic time scales for momentum, thermal, and species transport are $t_m \sim \delta_c^2/\nu \sim 5 \text{ s}$, $t_t \sim \delta_c^2/\alpha \sim 10 \text{ s}$, and $t_c \sim \delta_c^2/D \sim 1000 \text{ s}$. Within the liquid, we thus expect to decouple both momentum and thermal flow problems from the dominating CO₂ transport process. Subsequently, three primary assumptions are employed in this zeroth order analysis:

- First, by forming a ratio of air to liquid sorbent diffusive resistances, when CO₂ concentration boundary layers are of similar order, we find that $D\delta_a/D_a\delta_c \ll 1$, since typically $D_a \sim 10^{-5} \text{ m}^2/\text{s}$. We again find that the contactor CO₂ transport is liquid diffusion-dominated allowing the liquid flow problem to be further decoupled from the air flow problem.
- The second major assumption is that for long CO₂ diffusion times t_c , the liquid flow velocities are expected to be low, such that $\text{Re} \ll 1$, and liquid velocity distributions are quickly fully-developed and steady capillary meniscus profiles $h(z)$ are essentially linear and nearly flat.^{21,22} Temperature profiles are also quickly established and nearly uniform, since $t_m < t_t \ll t_c$.
- Thirdly, the capillary channels are slender such that $\delta^2/L^2 \ll 1$ allowing the 3-dimensional momentum equations to be approximated by the 1-dimensional z -component equation, where $\vec{u} = (0,0,w)$. Additionally, the wedge channels themselves are narrow such that $\alpha^2 \ll 1$, with shallow active depths ($\delta \approx H/3$) allowing them to be approximated as cartesian slots, where the span-flow area-averaged velocity is approximated as a function of x only, or even as a constant, where $w \approx w(x) \sim W$.

As a result, the liquid momentum equation may be decoupled from both the liquid species and heat transport equations such that the momentum, continuity, heat, and species transport equations (i.e., CO₂ and sorbent mixture constituents) may be solved analytically and in succession. Iterative and simultaneous solutions as well as full CFD simulations are pursued and will be reported at a later date. Most liquid sorbent property changes due to CO₂ absorption are slight (i.e., σ , ρ , and θ), allowing them to be assessed and addressed within the momentum and mass balances. However, sorbent viscosity μ , temperature, and water content may change significantly as CO₂ and water vapor are absorbed/desorbed. The model described above is based on a simple absorption process that is entirely physical or involves only weak chemical reactions (e.g. CO₂ in water). However, with minor modifications, it can be approximately applied to highly reactive sorbents, as discussed below.

For certain sorbents, the CO₂ transport in the liquid is governed by diffusion with local chemical reactions serving as a sink or source if either CO₂ is being desorbed (Contactor) or liberated (Degasser), respectively. In particular, primary amines (e.g., DGA) and secondary amines (e.g., DEA) chemically absorb CO₂ via the same reaction mechanism. The multi-step process that occurs is usually described via the zwitterion intermediate.²⁷ As an example, for DGA the chemical reactions involved in absorption of CO₂ into aqueous amine are



First, the amine group on the DGA binds to the CO₂, forming a zwitterionic intermediate. A base then deprotonates the zwitterion, forming a carbamate product. In an aqueous solution the base is water. In pure DGA the base is another molecule of DGA. The CO₂ also minimally reacts with water to form bicarbonate and carbonate. The rate of reaction of DGA with CO₂ is higher than the rate of diffusion of CO₂ into the liquid, thereby generating a sink for CO₂ absorption until all DGA is reacted, which sharpens the concentration gradient and improves the rate of CO₂ absorption by the liquid.

The strong chemical reaction can thus provide CO₂ uptake (both capacity and liquid-surface flux) that is several orders of magnitude greater than that of a physical sorbent.^{20,28} Hence, these liquids offer tremendous performance advantages.²⁹

In the model previously described, these characteristics can be crudely represented by a hypothetical aqueous physical sorbent with an enhanced solubility that can amplify the CO₂ concentration at the liquid surface (C_0) by several orders of magnitude. (e.g. $C_0 = 10^4 C_{ad}$). By doing so, we ultimately neglect the concentration sink/source term in the species transport equation. The potential for far greater CO₂ flux invalidates the previous molecular-diffusivity argument for negligible mass-transfer resistance within the gas phase. However, that condition can be reasonably reestablished by specifying a thin energetic *turbulent* boundary layer.

Additionally, the diffusio-chemical absorption/desorption of significant CO₂ (and water) will thus lead to unique volumetric changes within a reactive sorbent along the channels. Fortunately, for the momentum transport analysis, these volumetric changes in the sorbent upon CO₂ and water absorption/desorption may be addressed via known

analytical methods and by small volumetric source/sink terms added to the mass conservation equation within the momentum balance for the flow as will be shown.

B. Transport Equation Approximations

We first address the liquid sorbent momentum and mass conservation equations in reference to Fig. 4. In Fig 4a, an assumed uniform velocity enters the channel at $z = 0$ and the capillary free surface $h(z)$ adjusts due to pressure changes due to viscous resistance. The cartesian momentum equation for this flow is

$$\rho \bar{u}_t + \rho(\bar{u} \cdot \nabla) \bar{u} = -\nabla P + \mu \nabla^2 \bar{u} + \rho \bar{g}, \quad (3)$$

subject to mass/volume conservation equation $A_t = -Q_z \pm S$ (employing subscript notation for partial differentiation), where S is a source or sink term depending on thermal expansion, contraction, and absorption/desorption of CO_2 and water. Due to the low velocities expected, inertia is small such that $\mu L_{em}/\rho W \delta^2 \sin^2 \alpha \ll 1$ and the flow is essentially fully developed immediately. The same is true for the thermal entrance length, $\alpha_t L_{em}/W \delta^2 \sin^2 \alpha \ll 1$. For the small wedge channel dimensions, we find that $\text{Bo} = \rho g H^2 \tan^2 \alpha / \sigma \ll 1$ such that gravity effects can be neglected at zeroth order, especially in the reduced gravity environments aboard spacecraft. Thus, balancing capillary pressure with viscous resistance, Eq. (3) reduces to

$$P_z \approx \mu(w_{xx} + w_{yy}), \quad (4)$$

which may be solved to find^{21,22} that the average velocity and flow rate in the channels are

$$W \approx \frac{\sigma \Delta H}{3\mu f L} \quad \text{and} \quad Q \approx \frac{\sigma F_A \delta^2 \Delta H}{3\mu f L}, \quad (5)$$

respectively, where μ is the average viscosity for the temperature range expected. We note that for the narrow wedge section that approximately 70% of the flow rate is contained within a distance of approximately $0.3H$ from the free surface. For very low speed flows we find that $\Delta H \equiv H_1 - H_2$ is miniscule such that the free surface in Fig. 4a is essentially flat as depicted in Fig. 4b, where $h \approx H$. To be discussed, provided volumetric changes along the channel are low $SL/W\delta^2 \tan \alpha \ll 1$, $Q_1 \approx Q_2$ as sketched in Fig. 4. Thus, the flow rate in a single channel is $Q \approx F_A H^2 L / t_c$, with which we use in connection with Eq. (5) to determine ΔH .

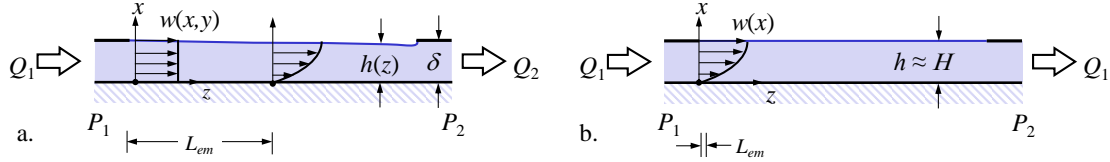


Figure 4. a. Developing flow with $h(z)$ and b. fully developed flow model with $h \approx H \sim \delta \approx H/3$.

Heat is conducted, convected, and generated within the liquid as it absorbs/desorbs CO_2 and moisture at the free surface. However, we note that thermal advection is small relative to axial conduction, such that $Wd^2 \sin^2 \alpha / \alpha L \ll 1$, where temperatures in the Contactor and Degasser are essentially uniform and constant. On the other hand, the steady species transport equation is

$$wC_z \approx D(C_{xx} + C_{zz}) \pm BC, \quad (6)$$

where B is the source/sink coefficient. We note that the source term may be ignored when $B\delta^2/D \ll 1$, that the flow is slender $\delta/L^2 \ll 1$ such that C_{zz} may be ignored, and since $W\delta^2/DL \sim 1$, the concentration entrance equation $WC_z \approx DC_{xx}$, subject to $C(x,0) \approx C_i$ and $C(\delta,z) \approx C_o$. Assuming $w \approx W$ from Eq. (5), we find the exact solution

$$C(x,z) = C_i + (C_o - C_i) \left\{ 1 - \sum_{m=1}^{\infty} \frac{4(-1)^{m+1}}{(2m-1)\pi} \exp \left[-\frac{(2m-1)^2 \pi^2}{4} \frac{Dz}{\delta^2 W} \right] \cos \left(\frac{(2m-1)\pi x}{\delta} \right) \right\}. \quad (7)$$

This CO_2 advection-diffusion problem is depicted in Fig. 5. Equation (7) identifies the effective entrance length for CO_2 saturation along the channel $L_{ec} \sim \delta^2 W/D \approx 1$ cm, which is the flow length for 91% average CO_2 saturation for the desired sorbent flow rate. With solutions such as Eqs. (5) and (7) and their respective constraints, we are now able to specify a LACR design assuming required CO_2 transport rates, CO_2 and water capacities of the fluids at Contactor and Degasser temperatures, and the temperature- and concentration-dependent thermophysical properties of the air and liquid sorbent flows for the environment operating conditions.

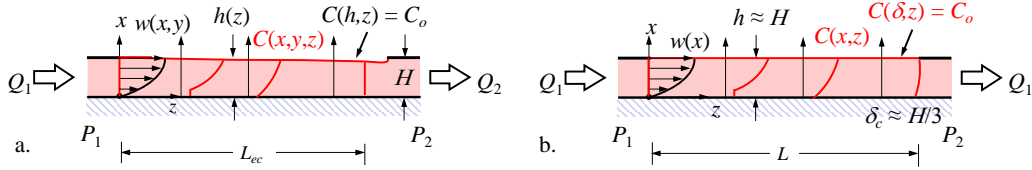


Figure 5. a. Concentration entrance problem with simplified model analyzed in b.

IV. LACR Design Guides

The LACR transport system design follows from specification of the CO₂ processing rate \dot{m} required of the target Contactor and Degasser environment temperatures, pressures, humidity, and CO₂ concentrations. It is then a question of liquid sorbent selection to meet the manifold performance requirements of quiet, stable, safe, small, lightweight, fast, low power, etc. Thus, the thermophysical properties of the sorbent are critical to a successful design. These include primarily temperature-, pressure-, and concentration-dependent density, viscosity, surface tension, contact angle, CO₂- and H₂O-diffusivity, and CO₂- and H₂O-capacity. Such data are readily available for amines such as MEA and DGA, but not necessarily so for all other liquids such as ionic liquids or ‘tox-zero’ ersatz candidates. Air-side CO₂ and H₂O transport properties are well established. We outline a typical design procedure for a Contactor here and provide suggestive sample quantitative values for a spacecraft application employing 65/35 DGA/Water as the liquid sorbent. The Degasser design is similar. With the thermophysical properties in hand, the LACR design proceeds in the following steps:

1. Choose wedge channel dimensions that meet stability requirements of given application—dimensions that prevent the liquid from ‘spilling out’ of the channels when perturbed. Assuming the channels are completely filled, there are three Bond number criteria used to guide this choice: for capillary dominance $Bo_R \equiv \rho a R^2 / \sigma \ll 1$, for overall channel stability $Bo_{RL} \equiv \rho a R L / \sigma \lesssim 1$, and for overall system stability $Bo_{RL_{sys}} \equiv \rho a R L_{sys} / \sigma \sim 1$, where $R = H \tan \alpha$. Dimensions R , L , and L_{sys} may be selected to meet these constraints producing highly stable interfaces, especially in the low-g environments of orbiting spacecraft. For our application we choose $R = 1$ mm and $L = L_{sys} = 10$ mm, leading to marginally stable conditions for terrestrial 1-g_o demonstration, but highly stable conditions for anything less (i.e., 100x FOS at 10⁻²g_o). Stability is dramatically increased for reduced liquid fill levels. We also note that viscous damping ($\mu L / \sigma R$) and natural frequencies ($\sigma / \rho R^3$)^{1/2} are high such that only DC g-levels are relevant, $\nu \ll 1$ Hz.
2. Select desired CO₂ concentration boundary layer penetration depth, δ_c . This is the depth of CO₂ penetration in the liquid desired to establish acceptable CO₂ concentration levels to meet overall CO₂ transport requirements. Too small and liquid delivery becomes challenging, too large and the time for saturation become excessive. We again note that the majority of the flow occurs near the free surface of the flow such that the lower 2/3 of the flow is relatively inactive from a transport point of view. Thus, an $H = 3$ mm deep narrow wedge channel provides an approximately 1 mm deep active region. Accordingly, we choose $\delta_c = 1$ mm ($\approx H/3$) due also due to practical 3-D print limitations.
3. Compute static CO₂ diffusion time, $t_c \approx \delta_c^2 / D$ (≈ 1000 s).
4. Compute capillary wedge channel flow characteristics providing liquid residence time t_c ; i.e., $w(x,y)$, H_2 , W , $Q = W F_A H^2$, and $\dot{m} \approx \rho F_A H^2 L / t_c$. Stable flows must not exceed jetting velocities $We \approx \rho W^2 R / \sigma < 1$, or ingestion flow²³ rate $Q_{ling} < (\mu L / 2 \rho \alpha^2) ((1 + Su^+)^{1/2} - 1)$, where $Su^+ \equiv \rho \sigma \alpha^3 H^3 / \mu^2 L^2$.
5. With knowledge of differing CO₂ concentrations between rich outlet and lean inlet streams, compute single channel CO₂ absorption ΔC (i.e., $\approx C_{50^\circ C} - C_{100^\circ C} \approx 114$ g CO₂/kg DGA).
6. Compute CO₂ uptake rate per channel $\dot{m}_c = \Delta C / t_c$.
7. Compute number n of channels needed to achieve the CO₂ requirement per crew member per day, = 1 kg CO₂/day-person, $\dot{m} = n \dot{m}_c$.
8. Apply margin. Due to the degree to which the primary assumptions of the flow are satisfied, the accuracy of these predictions is largely dependent on the accuracy of the fluid properties. A performance margin might be established assuming practical accommodations for non-ideal CO₂-air transport, undersaturation of exiting liquid at t_c (i.e., 91% saturated for 70% of flow), convection enhancements, enhancements for full accounting for curved free surface area, and second order impacts of volumetric liquid expansion along the channel. We currently estimate a margin of at least ≈ 3 needed to meet quantitative expectations of the system with a factor of safety of 2.

9. Compute total liquid flow rate Q_{tot} , total active area $A_{Contactor}$, Contactor/Degasser envelope estimates, etc.
10. Design manifold, air side ducting, fans, etc.
11. Compute total power required; i.e., heat $q = \dot{m}c_p\Delta T + \dot{m}_{H_2O}h_{fg}$, q_{pump} , q_{fan} , etc.

The order of these steps may vary and iterations are readily pursued to optimize certain parameters or groups of parameters. The LACR approach presents a system with attractive performance characteristics: silent, largely passive, stable, compact, with steady, nearly atmospheric pressure CO₂ delivery. Assuming spacecraft compatibility can be achieved, we find that to minimize the system power consumption we must minimize the liquid volume in circulation in the system as required in Eq. (1), which is achieved by ever thinner liquid films δ with ever higher CO₂ uptake capacities ΔC and diffusion rates D .

V. Outlook

We have described fundamental models influencing the design of a liquid sorbent, capillary-based system for transport and control of liquids, carbon dioxide uptake, and degasser power draw. Models for transport and control of liquids have been validated through microgravity experiments on the ISS (e.g. CSELS, etc.). Models for carbon dioxide uptake and degasser power draw will be validated in future ground and microgravity experiments. Steps are provided for applying the models for sizing a CO₂ scrubber system, including contactor/absorber, degasser, and other microgravity components as needed. This approach is being applied in the design of the ISS payload experiments that will serve to validate the models and sizing approach. The sizing approach will also be useful in the future comparison of the LACR approach to other CO₂ removal and storage systems.

The LACR project team is in the early stages of design and development, but the LACR Design Guide process has already provided insights:

1. Liquid sorbents can be stably contained and recirculated through a LACR system with considerable margin for fluid containment in microgravity conditions. Design guide rules drive the designs towards small flow channels with film thickness on the order of 1mm. Systems with simple corner wedges, and channels that provide film thickness on the order of 1mm are stable and contain the liquid under spacecraft conditions.
2. Liquid sorbent properties vary throughout the system, and this variability is driven primarily by temperature. The contactor and the degasser operate at different temperatures, and fluid data collected to date suggest that temperature changes dominate fluid variability. Initially, there were concerns that CO₂ uptake would change fluid volume to an extent that it impacts fluid flow. Available data suggests that volume change caused by CO₂ uptake has a negligible effect on fluid behavior compared to temperature effects.
3. Fluid velocity is set by chemical kinetics and film thickness. LACR designs are capable of recirculating fluids orders of magnitude faster than necessary. Even though capillary gradients drive the fluid flow and capillary gradients are relatively small, LACR designs have more than enough pumping capacity.
4. Total system size will be set by the film thickness, and film thickness will be set by manufacturing capability and practical considerations for filtering and fouling. Reference designs use channel depths on the order of 3mm and effective film thicknesses on the order of 1 mm. Improved manufacturing capabilities would enable thinner liquid films, lower quantities of recirculating liquid, and more compact CO₂ removal systems.

The LACR project team is developing a flight experiment system that can demonstrate fluid management of the LACR loop configuration and demonstrate fluid containment and loop recirculation for ambient temperature fluids in the contactor section and for elevated temperature fluids in the degasser section. To simplify the experiment, the first LACR flight experiment will use a liquid sorbent surrogate that is less toxic and has fewer restrictions for use on ISS. This experiment will measure fluid behavior in a recirculating loop that includes ambient and heated sections, and demonstrates control of a system with evaporation and loss of fluid volume in the degasser section, and stable performance across a wide range of fluid conditions. This LACR flight experiment is referred to as the ‘visible system’ because key elements of the system will be constructed in a way that fluid behavior can be visualized. Ground experiments will be run that correlate and compliment the data collected on ISS. If the LACR flight experiment and supporting ground experiments suggest that liquid sorbents can be used in a stable, silent, capillarity-driven CO₂ removal system that is substantially smaller than existing systems, the LACR project team will propose to develop a working CO₂ removal system based on capillary flow of a liquid sorbent.

Acknowledgments

This work was supported in part by NASA SBIR 2019-III Contract Number 80NSSC20C0004 through the Advanced Exploration Systems Program Life Support Systems Project. The authors also wish to thank the NASA

Innovative Advanced Concepts (NIAC) program for their sponsorship of the ‘Thirsty Walls’ project which enabled the first quantitative assessment of a recirculating liquid sorbent loop in a microgravity environment.

References

- ¹Matty, C. M., “Overview of Carbon Dioxide Control Issues During International Space Station/Space Shuttle Joint Docked Operations,” NASA Technical Reports Server, International Conference on Environmental Systems; July 11-15, 2010; Barcelona; Spain.
- ²Reysa, R.P., Lumpkin, J.P., El Sherif, D., Kay, R., Williams, D.E., International Space Station (ISS) Carbon Dioxide Removal Assembly (CDRA) Desiccant/Adsorbent Bed (DAB) Orbital Replacement Unit (ORU) Redesign., ICES 2007-01-3181, NASA. 2007 Orbital Replacement Unit (ORU) Redesign, International Conference on Environmental Systems, July 2007, Chicago.
- ³Knox, J., “Development of Carbon Dioxide Removal Systems for NASA’s Deep Space Human Exploration Missions 2017-2018.” 48th International Conference on Environmental Systems Proceedings, July 2018, ICES-2018-215.
- ⁴Isobe, J., Henson, P., MacKnight, A., Yates, S., Schuck, D., “Carbon Dioxide Removal Technologies for U.S. Space Vehicles: Past, Present, and Future.” 46th International Conference on Environmental Systems Proceedings, July 2017, ICES-2016-425, p.8.
- ⁵Yates, S., Kamire, R., Henson, P., Bonk, T., Loeffelholz, D., Zaki, R., “Scale-up of the Carbon Dioxide Removal by Ionic Liquid Sorbent (CDRILS) System,” 49th International Conference on Environmental Systems Proc., July 2019, ICES-2019-219.
- ⁶Torres, L., Jenson, R., Weislogel, M., “An ISS testbed approach to passive fluid phase separator device development for life support,” 49th International Conference on Environmental Systems Proceedings, July 2019, ICES-2019-199.
- ⁷Weislogel, M., Jenson, R., “Passive no moving parts capillary solutions for spacecraft life support systems,” 49th International Conference on Environmental Systems Proceedings, July 2019, ICES-2019-203.
- ⁸Wollman, A.P., “Large Length Scale Capillary Fluidics: From Jumping Bubbles to Drinking in Space,” Ph.D. Thesis, Portland State University, 2016
- ⁹Viestenz, K.J., Jenson, R.M., Weislogel, M.M., and Sargusingh, M.J., “Capillary Structures for Exploration Life Support Payload Experiment,” 48th International Conference on Environmental Systems, ICES-2018-241, 11 pages, 8-12 July 2018, Albuquerque, New Mexico.
- ¹⁰Turner, C., Goodman, J., Mohler, S., Mungin, R., Weislogel, M., Ungar, E., Buchli, J., “Mitigation of micro-droplet ejections during open cabin unit operations aboard ISS,” ICES-2019-201, 49th International Conference on Environmental Systems (ICES), Boston, 2019.
- ¹¹Vail, S., “Hazardous Materials Safety: An ISS Safety Review Panel (ISRP) Perspective”, POIWG October 22-24, 2019.
- ¹²Kelsey, L.K., Pasadilla, P., Fisher, J., and Lee, J., “Ionomer-membrane Water Processor (IWP) Engineering Development Unit (EDU) Brine Water Recovery Test Results,” 45th International Conference on Environmental Systems ICES-2015-124, 12-16 July 2015, Bellevue, Washington.
- ¹³Lowry, B.J. and Thiessen, D.B., “Fixed contact line helical interfaces in zero gravity,” *Physics of Fluids*, Volume 19, Issue 2, 022102 (2007) (12 pages).
- ¹⁴Graf, J., Cardin, K., and Torres, L., “Thirsty Walls: A New Paradigm for Air Revitalization in Life Support,” NASA Innovative Advanced Concepts, Fall Symposium, Oct. 22-25, 2015, Seattle.
- ¹⁵Jenson, R.M., Weislogel, M.M., Tavan, N.T., Chen, Y., Semerjian, B., Bunnell, C.T., Collicott, S.H., Klatte, J., Dreyer, M.E., “The Capillary Flow Experiments aboard the International Space Station: Increments 9—15, August 2004 to December 2007,” NASA/CR—2009-215586, September 2009.
- ¹⁶R.M. Jenson, A.P. Wollman, M.M. Weislogel, L. Sharp, R. Green, P.J. Canfield, J. Klatte, M.E. Dreyer (2014) Passive Phase Separation of Microgravity Bubbly Flows using Conduit Geometry, *Int. J. Multiphase Flow*, pp. 68-81, Final version published online: 24-JUN-2014, DOI information: 10.1016/j.ijmultiphaseflow.2014.05.011
- ¹⁷Maxwell, J.C., “Capillary Action, in the Scientific Papers of James Clerk Maxwell,” Cambridge Univ. Press, London, 1890.
- ¹⁸Collicott, S.H. and Weislogel, M.M., “Computation of Capillary Instabilities Using Surface Evolver,” *AIAA J.*, Vol. 42, No. 2, pp. 289-295, Feb. 2004.
- ¹⁹Sander, R., “Compilation of Henry’s Law Constants (Version 4.0) for Water as a Solvent,” *Atmos. Chem. Phys.*, Vol. 15, 2015, pp. 4399-4981.
- ²⁰Xu, Q. and Rochelle, G., “Total Pressure and CO₂ Solubility at High Temperature in Aqueous Amines,” *Energy Procedia*, Vol. 4, 2011, pp. 117-124.
- ²¹Weislogel, M.M. and Lichter, S., “Capillary Flow in Interior Corners,” *J. Fluid Mech.*, 373:349-378, November 1998.
- ²²Mohler, S., Weislogel, M., Graf, J., and Soto, L., “The Dynamics of Massively Parallel Open Capillary Channel Systems for Direct-Contact Liquid Sorbent Applications in Spacecraft Life Support,” ICES-2019-235, 49th International Conference on Environmental Systems (ICES), Boston, 2019.
- ²³Weislogel, M.M., Wollman, A.P., Jenson, R.M., Sharp, L.M., Geile, J.S., Tucker, J.F., Wiles, B.M., Trattner, A.L. DeVoe, C., Canfield, P.J., Klatte, J., Dreyer, M.E., “Capillary Channel Flow (CCF) EU2-02 on the International Space Station (ISS): An Experimental Investigation of Passive Bubble Separations in an Open Capillary Channel,” NASA/TM-2015-218720, June 2015 (68 pages).
- ²⁴SSP 57000, Pressurized Payloads, Revision S Interface Requirements Document, International Space Station Program Revision S, Type 4, January 2018.

²⁵McPherson, K., Kelly, E. and Keller, J., “Acceleration Environment of the International Space Station,” AIAA-2009-0957, (16 pages) AIAA 47th Aerospace Sciences Meeting, Orlando, FL, 5-8 January, 2009.

²⁶thruster firing [xx Ref.? xx]

²⁷Al-Juaied, M., and Rochelle, G., “Absorption of CO₂ in Aqueous Diglycolamine,” Industrial & Engineering Chemistry Research, Vol. 45, 2006, pp. 2473-2482

²⁸Li, L. and Rochelle, G., “CO₂ Mass Transfer and Solubility in Aqueous Primary and Secondary Amine,” Energy Procedia, Vol. 63, 2014, pp. 1487–1496.

²⁹Rogers, T., Paragano, M., Graf, J., Boerman, C., Belancik, G., Hogan, J., Jan, D., and Westover, S., “Selection and Characterization of a Liquid Sorbent for CO₂ Removal in Advanced Exploration Systems,” 47th International Conference on Environmental Systems Proceedings, July 2017, ICES-2017-123.